

Statistical Floquet prethermalization of the Bose-Hubbard model

Emanuele G. Dalla Torre^{1,2}

¹*Department of Physics, Bar-Ilan University, Ramat Gan 5290002, Israel*

²*Center for Quantum Entanglement Science and Technology,
Bar-Ilan University, Ramat Gan 5290002, Israel*

(Dated: November 8, 2021)

The manipulation of many-body systems often involves time-dependent forces that cause unwanted heating. One strategy to suppress heating is to use time-periodic (Floquet) forces at large frequencies. In particular, for quantum spin systems with bounded spectra, it was shown rigorously that the heating rate is exponentially small in the driving frequency. Recently, the exponential suppression of heating has also been observed in an experiment with ultracold atoms, realizing a periodically driven Bose-Hubbard model. This model has an unbounded spectrum and, hence, is beyond the reach of previous theoretical approaches. Here, we develop a semiclassical description of Floquet prethermal states and link the suppressed heating rate to the low probability of finding many particles on a single site. We derive an analytic expression for the exponential suppression of heating valid at strong interactions and large temperatures, which matches the exact numerical solution of the model. Our approach demonstrates the relevance of statistical arguments to Floquet prethermalization of interacting many-body quantum systems.

The study of periodically driven systems has a long history, tracing back to the work of Floquet in 1883 [1]. In the Floquet theory, the system is described by a time-independent unitary matrix, U_F , which captures the evolution over one period τ . Floquet theory can be used to solve classical systems only if they are governed by linear equations of motion. Remarkably, because the time evolution of quantum systems is determined by a linear equation (namely, the Schrödinger equation), this theory can be used to study any quantum system, even in the presence of interactions. The practical applicability of Floquet theory is hindered by the fact that finding U_F , and diagonalizing it, is generically very difficult. This difficulty is especially acute for many-body quantum systems, where the size of U_F grows exponentially with the number of degrees of freedom. At large driving frequencies, U_F can be derived using a controlled analytical approximation, the Magnus expansion [2]. The first term of this expansion is $U_F \approx e^{-iH_{av}\tau}$, where H_{av} is the time-averaged Hamiltonian. The other terms are integrals of commutation relations of the Hamiltonian at different times [3].

Using the Magnus expansion, Refs. [4–8] were able to obtain *rigorous* constraints on the time evolution of periodically driven quantum many-body systems. These rigorous theorems apply to quantum spin systems that satisfy a local norm bound: their Hamiltonians consist of sums of local operators whose matrix elements are smaller than a given energy scale J . For these systems, the heating rate Φ was shown to be exponential suppressed at large driving frequencies $\Omega = 2\pi/\tau$, according to

$$\Phi < \frac{AJ}{\hbar} \exp\left(-\frac{\hbar\Omega}{BJ}\right), \quad (1)$$

where \hbar is the Planck's constant, A and B are unitless constant. This exponential suppression was observed theo-

retically in a wide range of theoretical models [9–12] and in an experiment with dipolar spin chains [13].

The rigorous bound of Eq. (1) can be understood using a perturbative argument [4]: Due to the local norm bound, a single application of the driving field can change the energy of the system by J , at most. On the other hand, the absorption of a quantum of energy from the pump injects energy $\hbar\Omega$. Hence, the absorption of energy from the pump requires the product of $n = \hbar\Omega/J$ operators and is governed by the n th order perturbation theory. Refs. [5–8] used the Magnus expansion to extend this argument and demonstrate that Eq. (1) is a rigorous bound, valid to all orders. Interestingly, in the limit of $\hbar \rightarrow 0$, this bound applies to classical systems with a bounded spectrum [14, 15].

Many physical systems escape the regime of validity of the aforementioned rigorous bounds. For example, a massive particle with momentum p has a kinetic energy $p^2/2m$ that is unbounded from above. Ref. [16] demonstrated that systems of interacting particles can, nevertheless, show an exponential suppression of heating. They considered a canonical model of coupled kicked rotors [17–20] and showed that, for appropriate initial conditions, the system shows an exponentially long-lived prethermal plateau with vanishing energy absorption. This effect was explained in Ref. [21] using the following statistical argument: At large driving frequencies, the heating rate is small and the time-averaged energy of the system is (quasi) conserved. In this case, the system can be approximated by the Boltzmann distribution function

$$P = Z \exp\left(-\frac{H_{av}}{k_B T}\right), \quad (2)$$

where Z is the partition function, k_B is the Boltzmann constant, and T is the instantaneous temperature of the prethermal state, measured with respect to the average

Hamiltonian H_{av} . In the presence of other conserved quantities, such as the total momentum (or the total number of particles), the appropriate Lagrange multipliers need to be taken into account. The heating rate can, then, be estimated by the probability to incur into a many-body resonance [22]. Under physical assumptions, this probability is exponentially small, leading to a *statistical* Floquet prethermalization [21].

Having introduced the concepts of rigorous and statistical Floquet prethermalization, we now move to the focus of this manuscript, namely the periodically driven Bose-Hubbard model, described by

$$H(t) = \frac{U}{2} \sum_i n_i^2 - J(t) \sum_{\langle i,j \rangle} (b_i^\dagger b_j + H.c.), \quad (3)$$

with $J(t) = J_0 + \delta J \cos(\Omega t)$. Here, b_i and b_i^\dagger are canonical bosonic operators, $n_i = b_i^\dagger b_i$ is the number of particles on site i and $\langle i,j \rangle$ are nearest neighbors. The U term describes onsite repulsion and the J term hopping. Importantly, the U term is unbounded from above, making the rigorous bounds of Ref. [4–8] unapplicable. The Hamiltonian of Eq. (3) conserves the total number of particles in the system, $N = \sum_i n_i$. This model was recently realized in an experiment with ultracold atoms, where the time-dependent drive was induced by modulations of the laser fields that generate the optical lattice [23] [24].

Floquet prethermalization in the Bose-Hubbard model had been studied theoretically in Ref. [25] using a self-consistent quadratic approximation. This work employed the concept of many-body parametric resonance [26] to predict the existence of a frequency threshold above which the system does not absorb energy. However, in practice, terms that are neglected in the quadratic approximation lead to finite heating rates at all frequencies. Ref. [4] predicted that at large driving frequency, the heating rate should be rigorously bounded by a stretched exponential [27]. In the limit of an infinite number of particles per site, the model can be mapped to a system of classical rotors, where the heating rate is exponential suppressed [21].

Recently, the heating rate of the Bose-Hubbard model with one particle per site was studied by Ref. [23] using three methods: (i) the numerical calculation of the linear response of the model; (ii) the experimental measurement of single-site excitations (doublons or holes); (iii) the experimental measurement of the system's temperature. The experiments were performed in both one and two dimensions and were limited to relatively short times. Their findings demonstrated that the heating rate is exponentially suppressed as a function of Ω in all dimensions. As explained, this finding cannot be accounted by the available theoretical methods.

In this manuscript, we work in the framework of statistical Floquet prethermalization and develop a semiclassical model that captures the exponential suppression of

heating at strong interactions ($U \gg J$) and large temperatures ($T \gg J$). Following Ref. [21], we need to, first, identify the many-body resonances of the model. In the regime of large interactions, $U \gg J$, we can describe the system in terms of semiclassical particles hopping on a lattice. The periodic drive moves one particle from one site to a neighboring one. This process changes the value of the on-site interaction by

$$\begin{aligned} \Delta E &= \frac{U}{2} [(n_i \pm 1)^2 + (n_j \mp 1)^2] - \frac{U}{2} [(n_i)^2 + (n_j)^2] \\ &= U[\pm(n_i - n_j) + 1], \end{aligned} \quad (4)$$

where the upper (or lower) sign refers to a particle hopping from site j to site i (or *vice versa*). A resonance occurs when Eq. (4) equals to an integer multiple of the frequency of the drive (in units of Schrödinger's equation constant \hbar), or $\Delta E = m\hbar\Omega$, where m is an integer. For high-frequency drives, the heating rate is dominated by the lowest-order available resonance, which here corresponds to $m = \pm 1$. In what follows, we focus on the case where $n_\Omega = \hbar\Omega/U$ is integer and the resonance condition can be exactly matched. Furthermore, without loss of generality, we assume that $n_i > n_j$, such that when a particles moves from j to i (or *vice versa*) the interaction energy increase (decreases). The resonance condition $\Delta E = \pm\hbar\Omega$ becomes $\pm(n_i - n_j) + 1 = \pm n_\Omega$, or equivalently

$$n_j = n_i - n_\Omega \pm 1. \quad (5)$$

Here, the upper (or lower) sign refers to the absorption (or emission) of energy. Intuitively, at large driving frequencies ($n_\Omega \gg 1$), the resonance condition of Eq. (5) can be satisfied only by sites with a large number of particles ($n_i \geq n_\Omega \gg 1$). Because the probability to find these sites is exponentially small, so is the probability to absorb a photon from the cavity, leading to suppressed heating rates. The goal of this manuscript is to put this intuitive argument on solid mathematical ground.

The probability to satisfy the resonance condition of Eq. (5) is determined by $P_{i,j}(n_i, n_j)$, the joint distribution function to find n_i and n_j particles in sites i and j , according to

$$P_\pm(\Omega) = \sum_n P_{i,j}(n, n - n_\Omega \pm 1). \quad (6)$$

This expression needs to be multiplied by a factor of 2 to take into account the case of $n_i < n_j$. In a d dimensional lattice, we need to further multiply the result by the coordination number d [28].

Evaluating the distribution function $P_{i,j}(n_i, n_j)$ in a (pre)thermal state described by Eq. (2) is a formidable task in many-body quantum physics. In the present manuscript we are interested in large temperatures $T \gg J$, where we can neglect quantum fluctuations and describe the prethermal state by

$$P_{i,j}(n_i, n_j) = P_i(n_i)P_j(n_j), \quad (7)$$

with

$$P_i(n) = P_j(n) = Z_0 \exp\left(-\frac{U}{2k_B T} n^2 - \frac{\mu}{k_B T} n\right). \quad (8)$$

Here, in addition to the quasi-conservation of the energy in the prethermal state, we took into consideration the conservation of the total number of particles, through the chemical potential μ . The values of Z_0 and μ are determined by the constraints $\sum_n Z_i(n) = 1$ and $\sum_n n Z_i(n) = \bar{n}$, where \bar{n} is the average number of particles per site (often referred to as filling).

These constraints, along with the numerical solution of Eqs. (6)-(8) enable us to compute the semiclassical heating rate of the Bose-Hubbard model, Φ . The total heating rate is given by the probability to incur into a resonance ($P_+ - P_-$), times the heating rate of an individual resonance. According to the linear response theory, one obtains

$$\Phi(\Omega) = (\delta J)^2 (P_+ - P_-) \delta(\Omega - \Delta E), \quad (9)$$

Here, the delta function $\delta(\Omega - \Delta E)$ imposes the relevant resonance condition. For finite J/U , this function is broadened by the single-particle bandwidth and can be approximated by a square function of width $4J$, namely $\delta(\omega) = [\Theta(\omega > -2J) - \Theta(\omega > 2J)]/(4J)$, where Θ is the Heaviside function. The heating rates resulting from the numerical solution of our semiclassical approach, Eq. (6)-(9), are shown in the upper panel of Fig. 1, for different values of the temperature. For clarity, we plotted the function Φ for integer values of U/\hbar only [29]. We find that the heating rate is exponentially suppressed for all temperatures and, at large temperatures, inversely proportional to the temperature.

To gain physical insight into this result, we now develop an analytical high-temperature expansion. In the limit of $T \rightarrow \infty$, the distribution function is solely determined by the conservation laws and

$$P_i(n) = Z_0 \exp\left(-\frac{\mu n}{k_B T}\right) \equiv Z_0 z^n \quad (10)$$

with $Z_0 = 1 - z$ and $z = \bar{n}/(1 + \bar{n})$ [30]. By combining Eqs. (6) and (10), we obtain

$$P_+ = (1 - z)^2 \sum_{n=n_\Omega}^{\infty} z^{2n-n_\Omega+1} = \frac{1-z}{1+z} z^{\hbar\Omega/U+1} \quad (11)$$

$$P_- = (1 - z)^2 \sum_{n=n_\Omega+1}^{\infty} z^{2n-n_\Omega-1} = \frac{1-z}{1+z} z^{\hbar\Omega/U+1}. \quad (12)$$

Note that the two sums have different lower limits because P_+ can occur only if $n_j \geq 1$, while P_- requires only $n_j \geq 0$. Because $P_+ = P_-$ the net energy absorption is zero, $\Phi = 0$. This result is not surprising: infinite temperature ensembles do not absorb energy!

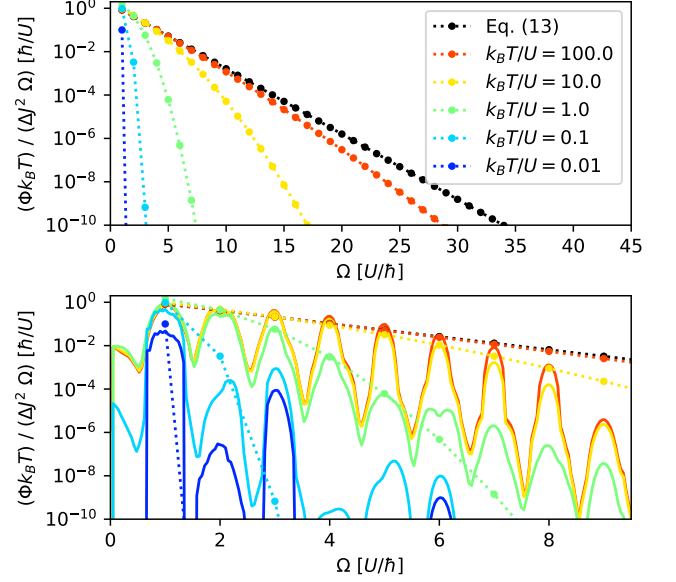


FIG. 1. **Heating rate of the Bose-Hubbard model at filling $\bar{n} = 1$ for $J/U = 0.05$.** Dotted curves: semiclassical approximation based on Eqs. (6) - (8) and its high-temperature expansion, Eq. (15). Continuous curves: exact diagonalization of the Bose-Hubbard model at $J/U = 0.02$. At temperatures $T \gtrsim U$, the results of the two approaches coincide.

We can use this result as the starting point of a perturbative analysis. By approximating Eq. (8) as $P \approx Z_0 (1 - U n^2/(2k_B T)) e^{-\mu n}$ [31] we obtain

$$P_{\pm} = Z_0^2 \sum_{n_i - n_j = n_\Omega \pm 1} \left[1 - \frac{U}{2k_B T} (n_i^2 + n_j^2) \right] z^{n_i} z^{n_j}, \quad (13)$$

leading to (see symbolic script in appendix B)

$$P_+ - P_- = \frac{\hbar\Omega}{k_B T} \frac{1-z}{1+z} z^{\hbar\Omega/(hU)+1}. \quad (14)$$

In particular, at unit filling $\bar{n} = 1$ ($z = 1/2$), we obtain

$$\Phi = \frac{(\delta J)^2 \hbar\Omega}{12 J k_B T} \exp\left(-\log(2) \frac{\hbar\Omega}{U}\right). \quad (15)$$

This equation synthesizes our two main results: at large temperatures, the heating rate of the Bose-Hubbard model is an exponential function of the ratio between the driving frequency and the onsite interaction and is inversely proportional to the temperature.

We now compare the results of our semiclassical approximation with the exact diagonalization of the Bose-Hubbard model. At finite temperatures, linear response

gives [23]

$$\Phi = \frac{\delta J^2}{2L} \sum_{m,n} |\langle \psi_n | V | \psi_m \rangle|^2 \delta(E_n - E_m - \hbar\Omega) \times \frac{1}{Z} \left(e^{-E_m/k_B T} - e^{-E_n/k_B T} \right). \quad (16)$$

Here $|\psi_n\rangle$ and E_n are, respectively, the eigenstates and eigenvalues of the average Hamiltonian H_{av} at filling $\bar{n} = 1$ and $V = \sum b_i^\dagger b_j + H.c.$ is the time-dependent perturbation. We evaluate this quantity numerically for $N = 9$ particles on an open chain with $L = 9$ sites, using the QuSpin package [32, 33], see appendix C [34]. In our numerical calculations, we used the above-mentioned square function to broaden the resonances and mitigate the finite dimension of the lattice. Because the maximal number of particles per site is always smaller or equal to the total number of particles N , we need to restrict ourselves to frequencies Ω , such that $n_\Omega < N$, or $\hbar\Omega < NU$ [35]. As shown in the lower panel of Fig. 1, for all temperatures $T > U$ the resulting curves precisely match the semiclassical approximation.

At low temperatures, $T < U$, the heating rate is affected by additional *quantum* resonances. In particular, at driving frequencies $3U/\hbar$ and $6U/\hbar$ the heating rate is significantly higher than the one predicted by the semiclassical approximation. These resonances are due to processes that involve the hopping of more than one particles, such as the creation of triplons and quadruplons [23]. These processes are classically forbidden because the perturbation V hops a single particle, but can acquire a finite probability due to the quantum coherence between states with different occupation numbers. The corresponding heating rate is proportional to high powers of J/U and are, hence, subdominant with respect to the semiclassical processes described by Eq. (15).

To summarize, in this manuscript we discussed the differences between rigorous [4–8] and statistical [21] Floquet prethermalization. The former approach relies on the boundedness of quantum operators and applies to spin models only. See also Ref. [36], where it was shown that the rigorous approach applied to systems of interacting particles with an unbounded spectrum does not lead to exponential bounds on diffusion rates. The latter approach relies on the statistical description of the prethermal state and applies to a wider range of models. A key difference between these two approaches is that, while the rigorous approach is independent on the initial state, the statistical approach depends on the initial state, through its (quasi)conserved quantities, such as energy and particles' number.

Here, we applied the statistical argument to the periodically driven Bose-Hubbard model, which was recently realized experimentally [23]. We developed a semiclassical approximation, valid in the regime of strong interactions and large temperatures ($U > k_B T \gg J$), and used

it to derive an analytical expression for the heating rate Φ . This expression is found to match the results of the exact diagonalization with no fitting parameter. Importantly, we demonstrated that in this regime, the exponential suppression of the heating does not depend on dimensionality and persists at all temperatures. In this latter aspect, the Bose-Hubbard model differs from the coupled rotors model of Refs. [16–21], where the exponential suppression of heating disappears at large temperatures, eventually leading to a runaway from the prethermal regime. This fundamental difference stems from the nature of the conserved quantities of the two models: In the rotor model, the conserved quantity, namely the momentum of the rotors p_i , is a continuous variable and can acquire both positive and negative values. At large temperatures, the fluctuations of p_i diverge making the exponential suppression of heating ineffective. In contrast, in the Bose-Hubbard model, the conserved quantity, namely the particles' number n_i , is non-negative. If the expectation value of n_i is kept fixed, the fluctuations of this quantity remain finite and the heating rate is suppressed at all temperatures. The prediction of the two models coincide when the average number of particles per site is taken to infinity.

We thank Jonathan Ruhman, Francois Huveneers, and the authors of Ref. [23] for useful discussions. This work was supported by the Israel Science Foundation, Grants No. 151/19 and 154/19.

-
- [1] G. Floquet. *Sur les équations différentielles linéaires à coefficients périodiques*. In *Annales scientifiques de l'École normale supérieure*, volume 12, pages 47–88 (1883).
 - [2] W. Magnus. *On the exponential solution of differential equations for a linear operator*. Communications on pure and applied mathematics 7 (4), 649 (1954).
 - [3] See, for example, Ref. [37] for an introduction.
 - [4] D. A. Abanin, W. De Roeck, F. Huveneers. *Exponentially slow heating in periodically driven many-body systems*. Physical Review Letters 115 (25), 256803 (2015).
 - [5] T. Mori, T. Kuwahara, K. Saito. *Rigorous bound on energy absorption and generic relaxation in periodically driven quantum systems*. Physical Review Letters 116 (12), 120401 (2016).
 - [6] D. Abanin, W. De Roeck, W. W. Ho, F. Huveneers. *A rigorous theory of many-body prethermalization for periodically driven and closed quantum systems*. Communications in Mathematical Physics 354 (3), 809 (2017).
 - [7] D. A. Abanin, W. De Roeck, W. W. Ho, F. Huveneers. *Effective Hamiltonians, prethermalization, and slow energy absorption in periodically driven many-body systems*. Physical Review B 95 (1), 014112 (2017).
 - [8] T. Mori, T. N. Ikeda, E. Kaminishi, M. Ueda. *Thermalization and prethermalization in isolated quantum systems: a theoretical overview*. Journal of Physics B: Atomic, Molecular and Optical Physics 51 (11), 112001 (2018).

- (2018).
- [9] S. A. Weidinger, M. Knap. *Floquet prethermalization and regimes of heating in a periodically driven, interacting quantum system*. Scientific reports 7 (1), 1 (2017).
 - [10] D. V. Else, B. Bauer, C. Nayak. *Prethermal phases of matter protected by time-translation symmetry*. Physical Review X 7 (1), 011026 (2017).
 - [11] F. Machado, G. D. Kahanamoku-Meyer, D. V. Else, C. Nayak, N. Y. Yao. *Exponentially slow heating in short and long-range interacting floquet systems*. Physical Review Research 1 (3), 033202 (2019).
 - [12] K. Mallayya, M. Rigol. *Heating rates in periodically driven strongly interacting quantum many-body systems*. Physical Review Letters 123 (24), 240603 (2019).
 - [13] P. Peng, C. Yin, X. Huang, C. Ramanathan, P. Cappelaro. *Observation of floquet prethermalization in dipolar spin chains*. arXiv preprint arXiv:1912.05799 (2019).
 - [14] O. Howell, P. Weinberg, D. Sels, A. Polkovnikov, M. Bukov. *Asymptotic prethermalization in periodically driven classical spin chains*. Physical Review Letters 122 (1), 010602 (2019).
 - [15] T. Mori. *Floquet prethermalization in periodically driven classical spin systems*. Physical Review B 98 (10), 104303 (2018).
 - [16] A. Rajak, R. Citro, E. G. Dalla Torre. *Stability and prethermalization in chains of classical kicked rotors*. Journal of Physics A: Mathematical and Theoretical 51 (46), 465001 (2018).
 - [17] K. Kaneko, T. Konishi. *Diffusion in Hamiltonian dynamical systems with many degrees of freedom*. Physical Review A 40 (10), 6130 (1989).
 - [18] T. Konishi, K. Kaneko. *Diffusion in Hamiltonian chaos and its size dependence*. Journal of Physics A: Mathematical and General 23 (15), L715 (1990).
 - [19] B. Chirikov, V. Vecheslavov. *Arnol'd diffusion in large systems*. Journal of Experimental and Theoretical Physics 85 (3), 616 (1997).
 - [20] M. Mulansky, K. Ahnert, A. Pikovsky, D. L. Shepelyansky. *Strong and weak chaos in weakly nonintegrable many-body Hamiltonian systems*. Journal of Statistical Physics 145 (5), 1256 (2011).
 - [21] A. Rajak, I. Dana, E. G. Dalla Torre. *Characterizations of prethermal states in periodically driven many-body systems with unbounded chaotic diffusion*. Physical Review B 100 (10), 100302 (2019).
 - [22] B. V. Chirikov. *A universal instability of many-dimensional oscillator systems*. Physics Reports 52 (5), 263 (1979).
 - [23] A. Rubio-Abadal, M. Ippoliti, S. Hollerith, D. Wei, J. Rui, S. Sondhi, V. Khemani, C. Gross, I. Bloch. *Floquet prethermalization in a bose-hubbard system*. arXiv preprint arXiv:2001.08226 (2020).
 - [24] Note that this modulation makes U time dependent as well and, for small $\delta J/J_0$, the relative oscillations of U and J are comparable.
 - [25] M. Bukov, S. Gopalakrishnan, M. Knap, E. Demler. *Prethermal Floquet steady states and instabilities in the periodically driven, weakly interacting bose-hubbard model*. Physical review letters 115 (20), 205301 (2015).
 - [26] R. Citro, E. Dalla Torre, L. D'Alessio, A. Polkovnikov, M. Babadi, T. Oka, E. Demler. *Dynamical stability of a many-body Kapitza pendulum*. Annals of Physics 360, 694 (2015).
 - [27] To the best of our knowledge, the proof of this claim is not publicly available.
 - [28] According to our approach, the dimensionality does not affect the exponential suppression of the heating rate, in agreement with the experimental observations of Ref. [23]. This is in contrast to their theoretical expectation, where the rigorous approach is used to derive a stretched exponential with exponent of the form $\exp(\Omega^\alpha)$ with $\alpha = (1 + d)/2d$.
 - [29] The script used to generate this figure is given in Appendix A.
 - [30] Eq. (10) can be formally derived by considering Eq. (8) in the limit $T \rightarrow \infty$, at a fixed μ/T , such that $U \ll T$ can be neglected.
 - [31] Here we are neglecting the corrections due to the renormalization of the partition function, Z_0 . These corrections are identical in P_+ and P_- and cancel out.
 - [32] P. Weinberg, M. Bukov. *Quspin: a python package for dynamics and exact diagonalisation of quantum many body systems part i: spin chains*. SciPost Phys 2 (003) (2017).
 - [33] P. Weinberg, M. Bukov. *Quspin: a python package for dynamics and exact diagonalisation of quantum many body systems. part ii: bosons, fermions and higher spins*. SciPost Phys. 7 (arXiv: 1804.06782), 020 (2019).
 - [34] The exact diagonalization was performed using QuSpin version 0.3.3 for Python2.7 on a personal computer with an Intel core i7 (8th generation) CPU and 24 GB RAM. The script used to generate Fig. 1 is given in appendix C and required approximately 2 seconds, 30 seconds, 15 minutes, 6 hours for $N = L = 6, 7, 8, 9$, respectively.
 - [35] Finite size effects are further studied in Appendix D, where we show the results of the calculation for $N = 7$ and $N = 8$ particles.
 - [36] F. Huveneers, J. Lukkarinen. *Pre-thermalization in a classical phonon field: slow relaxation of the number of phonons*. arXiv preprint arXiv:2002.10868 (2020).
 - [37] M. Bukov, L. D'Alessio, A. Polkovnikov. *Universal high-frequency behavior of periodically driven systems: from dynamical stabilization to Floquet engineering*. Advances in Physics 64 (2), 139 (2015).

Appendix

A. Matlab script used to plot the semiclassical approximation in Fig. 1

```

1  close all; clear all
2  syms n; syms U; syms mu
3
4  %Temperature is set to one
5  H = U*n^2/2 + mu*n
6  myUs=logspace(-log10(100),-log10(0.01),5)
7  %myUs=logspace(-3,0,4)
8
9  %myUs=myUs(length(myUs):-1:1)
10
11 Nmax=60;
12
13 PP=zeros(length(myUs),Nmax*2/3);
14
15 for u=1:length(myUs)
16     myU=myUs(u)
17     Z = @(mymu) sum(double(subs(exp(-subs(subs(H,U,myU),mu,mymu)),n,0:Nmax)));
18     avn = @(mymu) sum(double(subs(n*exp(-subs(subs(H,U,myU),mu,mymu)),n,0:Nmax)));
19     avn2 = @(mymu) sum(double(subs(n^2*exp(-subs(subs(H,U,myU),mu,mymu)),n,0:Nmax)));
20     ;
21     eqn = @(mymu) avn(mymu)/Z(mymu)-1;
22
23     mymu = fzero(eqn,1)
24     myavn2(u)= avn2(mymu)/Z(mymu)
25     P=exp(-subs(subs(H,U,myU),mu,mymu));
26
27     figure(2)
28     semilogy(subs(P,n,0:Nmax));
29     hold on
30     mylegend{u}=[ 'k_BT/U=', num2str(1/myU) ];
31
32     allP=double(subs(exp(-subs(subs(H,U,myU),mu,mymu)),n,0:Nmax))/Z(mymu);
33
34     for nOmega=1:(Nmax*2/3)
35         nn=nOmega:Nmax;
36         Pplus=sum(allP(1+nn).*allP(1+nn-nOmega+1));
37         %add 1 because the first item of allP corresponds to n=0;
38         nn=(nOmega+1):Nmax;
39         Pminus=sum(allP(1+nn).*allP(1+nn-nOmega-1));
40         PP(u,nOmega)=2*(Pplus-Pminus);
41     end
42
43     figure(3)
44     semilogy([0,1:(Nmax*2/3)], [0,PP(u,:)/myU.*(1:Nmax*2/3)], 'linewidth',1.0, 'marker',
45         ' ','markersize',15.0)
46     hold on;
47 end
48 save('PP.mat','PP','myUs');
```

```

49 nn=0:Nmax;
50 plot(nn,nn.^2.*exp(-log(2)*nn)/3,'k—','linewidth',1.0,'marker','.', 'markersize',
    ,15.0);
51 mylegend{u+1}='Eq. (13)';
52 rubio %plots the inset of Fig. 7 of Ref. [22] (v2)
53
54 xlabel('$\{\it \Omega\}^{\sim}[U/\hbar]$', 'Interpreter', 'latex');
55 ylabel('$\{\Phi\}^{\it k\_B T\}^{\sim}[U^2/\hbar]$', 'Interpreter', 'latex');
56 xlim([0,45]);ylim([1E-8,1]);
57
58 set(gca,'fontname','times');
59 set(gca,'fontsize',12);
60 set(gca,'xtick',0:10:50);
61 set(gca,'ytick',10.^(-8:2:0));
62 legend(mylegend,'location','northeast','box','off','fontsize',10)
63
64 set(gcf,'color','white');
65 set(gcf,'position',[100 100 500 300]);
66 saveas(gcf,'numerics.eps','eps')

```

B. Matlab symbolic script used to derive Eqs. (11), (12), and (14)

```

1 syms a; syms n; syms nOmega
2 assume(a>0 & a<1)
3
4 symsum(a^n,n,0,Inf)
5 simplify((1-a)^2*symsum(a^(2*n-nOmega+1),n,nOmega,Inf))
6 simplify((1-a)^2*symsum(a^(2*n-nOmega-1),n,nOmega+1,Inf))
7 Pplus=(1-a)^2*symsum((n^2+(n-nOmega+1)^2)*a^(2*n-nOmega+1),n,nOmega,Inf)
8 Pminus=(1-a)^2*symsum((n^2+(n-nOmega-1)^2)*a^(2*n-nOmega-1),n,nOmega+1,Inf)
9 simplify(Pplus-Pminus)

```

C. Python script used to plot the exact diagonalization in Fig. 1

```

1 #Study the temperature dependence of the heating rate in the Bose–Hubbard model
2
3 from __future__ import print_function, division
4 import sys,os
5 import scipy.io as spio
6 import seaborn as sns
7
8 from quspin.operators import hamiltonian # Hamiltonians and operators
9 from quspin.operators import quantum.LinearOperator # operators
10 from quspin.basis import boson-basis_1d # bosonic Hilbert space
11 import time
12 import numpy as np # general math functions
13 import matplotlib.pyplot as plt # plotting library
14 #
15 #plt.rcParams["font.family"] = "Times New Roman"
16
17 ##### define model parameters
18 # initial seed for random number generator
19 np.random.seed(0) # seed is 0 to produce plots from QuSpin2 paper
20 # setting up parameters of simulation
21 L = 8 # length of chain
22 N = L # number of sites
23 nb = 1 # density of bosons

```

```

24 sps = L+1 # number of states per site
25
26 J_par = 0.05; U = 1.0; gamma=2*J_par; Emax=9.5; Nomega=200;mylim=[1e-10,2];allT
    =[100,10,1,0.1,0.01];unit='U';PBC=False
27
28 plt.figure(1,figsize=(5,5))
29 sp=sns.color_palette('jet_r',5);#dark#rainbox
30 plt.subplot(212)
31
32 ##### Numerics: Diagonalizing Hamiltonian
33 filename = "/data/ED3-JoU"+str(J_par/U)+"_N"+str(N)+"_PBC"+str(PBC)
34 if not os.path.exists(filename+"allE.npy") :
35     print("Running",filename)
36     tic=time.time()
37     ##### set up Hamiltonian and observables
38     int_list_1 = [[-0.5*U,i] for i in range(N)] # interaction  $-\frac{U}{2} \sum_i n_i$ 
39     int_list_2 = [[0.5*U,i,i] for i in range(N)] # interaction:  $\frac{U}{2} \sum_i n_i^2$ 
40     if PBC :
41         hop_list = [[-J_par,i,(i+1)%N] for i in range(0,N,1)] # PBC
42     else :
43         hop_list = [[-J_par,i,i+1] for i in range(0,N-1,1)] # OBC
44     hop_list_hc = [[J.conjugate(),i,j] for J,i,j in hop_list] # add h.c. terms
45     # set up static and dynamic lists
46     static = [
47         ["+",hop_list], # hopping
48         ["+",hop_list_hc], # hopping h.c.
49         ["nn",int_list_2], #  $\sum_i n_i^2$ 
50         ["n",int_list_1] #  $-\sum_i n_i$ 
51     ]
52
53     #Note that "perturbation" is proportional to J_par —> need to divide Phi by
        J_par**2
54     perturbation = [
55         ["+",hop_list], # hopping
56         ["+",hop_list_hc] # hopping h.c.
57     ]
58     dynamic = [] # no dynamic operators
59
60     basis = boson_basis_1d(N,nb=nb,sps=sps)
61     print("total H-space size: {}".format(basis.Ns))
62
63     HBHM = hamiltonian(static,dynamic,basis=basis,dtype=np.complex128)
64     allE,allV=HBHM.eigh()
65     hop=hamiltonian(perturbation,dynamic,basis=basis,dtype=np.complex128)
66     matrix_elem2=np.power(np.abs((hop.rotate_by(allV,generator=False)).toarray()),2)
        ;
67
68     np.save(filename+"allE.npy",allE)
69     np.save(filename+"me.npy",matrix_elem2)
70     toc=time.time();print("Time : ",toc-tic)
71
72 else :
73     print('Loading',filename)
74     allE=np.load(filename+"allE.npy")
75     matrix_elem2=np.load(filename+"me.npy")
76

```



```

77
78 ##### Numerics: Computing the spectrum
79 allomega=np.linspace(0,Emax,Nomega);
80
81 for c in range(len(allT)):
82
83     T=allT[c]
84     tic=time.time()
85     filename2 = filename+"_T"+str(T)+"_gamma"+str(gamma)+"_Emax"+str(Emax)+"_Nomega"
86         +str(Nomega)
87
88     if not os.path.isfile(filename2+".npy") :
89         print('Running ',filename2)
90         allPhi=np.zeros(Nomega);
91
92         Ej,Ek = np.meshgrid(allE , allE );
93
94         Z=np.sum(np.exp(-(allE-allE[0])/T));
95         Pj = np.exp(-(Ej-allE[0])/T)/Z;
96         Pk = np.exp(-(Ek-allE[0])/T)/Z;
97
98         P0 = (Pk-Pj)*matrix_elem2
99         for w in range(Nomega) :
100             deltaE=Ej-Ek-allomega[w]
101             allPhi[w]=np.sum((P0*(deltaE<gamma)*(deltaE>gamma)/gamma/2))
102
103         toc=time.time()
104         print("Time:",toc-tic)
105         np.save(filename2+".npy",allPhi);
106     else :
107         print('Loading ',filename2)
108         allPhi=np.load(filename2+".npy");
109
110     plt.semilogy(allomega,T*allPhi/(1e-15+allomega)/J_par**2/L/2,label="T/U= "+str(T)
111         ),color=sp[c]);#sp(colori[c]));
112
113 ##### Semiclassical approximation (laoding from Matlab)
114 mat = spio.loadmat(' ../PP.mat', squeeze_me=True)
115 PP=mat['PP']
116 myUs=mat['myUs']
117 print('Loaded theory for T/U',1/myUs)
118 sh=PP.shape
119 Nmax=sh[1];
120
121 for s in [1,2]:
122     ax=plt.subplot(210+s)
123     nn=np.array(range(1,45))
124     plt.semilogy(nn,1/3*np.power(1/2,nn/U)/2/gamma,'k.: ',label="Eq. (13)")
125     nn=np.array(range(1,Nmax+1))
126     for i in range(sh[0]) :
127         plt.semilogy(nn,PP[i,:]/myUs[i]/nn/2/gamma,'.: ',label=r'$k_B T/$'+unit+'='+
128             str(1/myUs[i])+"$") ,color=sp[i]);#sp(colori[i]));
129     plt.xlabel(r"$\Omega$ [" +unit+" / $\hbar$]");
130     plt.ylabel(r"$\left(\Phi_{k_B T}\right) / (\Delta J^2 \Omega) [\hbar /$"+unit+"
131         ]$");

```

```

129     box = ax.get_position()
130     print(box)
131     plt.ylim(mylim);
132     ax.set_position([box.x0+0.05*box.width, box.y0+0.05*box.height*(3-s), box.width,
133                     0.95*box.height])
134     plt.yticks([1e-10,1e-8,1e-6,1e-4,1e-2,1])
135 plt.subplot(211)
136 plt.xlim([0,Nmax+5]);
137 plt.legend(loc=1)
138 plt.subplot(212)
139 plt.xlim([0,Emax]);
140 plt.savefig("../"+filename[5:]+".pdf")
141 plt.show()

```

D. Finite size effects

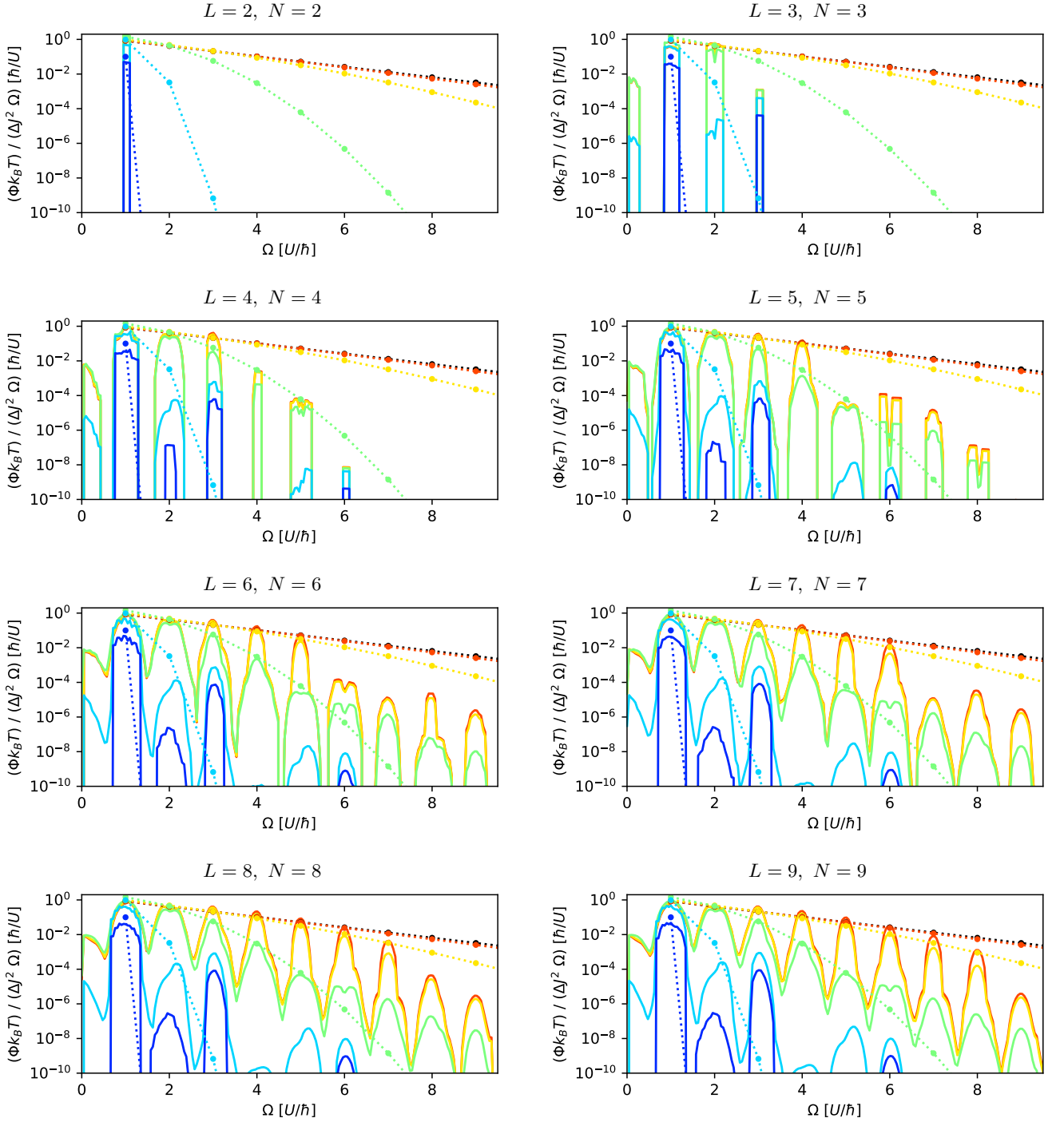


FIG. 2. Same as the lower panel of Fig. 1 for N particles on L sites. No fitting parameter is used. The semiclassical approximation matches the exact results for frequencies $\hbar\Omega < N/U$ and temperatures $k_B T > U$.